INTERNATIONAL JOURNAL OF CONSERVATION SCIENCE
ISSN: 2067-533X Volume 15, Issue 3, 2024: 1523-1532 www.ijcs.ro
DOI: 10.36868/IJCS.2024.03.23

MODELLING THE IMPACT OF SOIL AND METEOROLOGICAL PARAMETERS ON CARBON DYNAMICS IN WETLAND ECOSYSTEMS

Natalia ENACHE[1,2], György DEÁK[1,3,*], Lucian LASLO[1], Monica MATEI[1], Elena HOLBAN[1], Madalina BOBOC[1], Alexandra HARABAGIU[1,2]

[1]Department of Climate Change and Sustainable Development, National Institute for Research and Development in Environmental Protection (INCDPM), 060031 Bucharest, Romania.
[3]Doctoral School of Biotechnical Systems Engineering, University POLITEHNICA of Bucharest, – Splaiul Independenței 313, District 6, 060042 Buchares, Romania
[2]Doctoral School of Biotechnical Systems Engineering, University POLITEHNICA of Bucharest, Splaiul Independenței 313, District 6, 060042 Buchares, Romania

Abstract

Wetlands are characterised by distinct hydrological regimes and have significant importance in the global carbon cycle, having the potential to reduce carbon emissions through long-term carbon storage in the soil. In this study, carbon dynamics were simulated using a process-based model DeNitrification-DeComposition (DNDC), for two locations along Dâmbovița River case study area. These scenarios took into consideration the interconnection of soil parameters, hydrology, meteorological conditions and vegetation type. The findings showed that soil CO_2 emissions are positively and strongly correlated with air temperature and soil moisture, with changes in the water content of the soil regime having the greatest impact on CO_2 fluxes. Also, the model simulations have been validated by statistical analysis of uncertainties with the values of CO_2 fluxes measured in situ using the dynamic closed chamber method. By comparing DNDC outputs with field measurements, the performance of the model was evaluated in different environmental conditions and the results were consistent, which increased confidence in its application for assessing wetland ecosystems. These results contribute to a more comprehensive understanding of the carbon cycle in wetlands and an improved estimation of the effects of climate change on the dynamics of carbon in these ecosystems.

Keywords*: DNDC; Model evaluation; CO_2 fluxes; Greenhouse gases; Climate change*

Introduction

Among the most complex ecosystems are wetlands, which have significance in the global cycling of carbon dioxide and climate management. The processes by which wetlands absorb carbon and how environmental changes influence CO_2 emissions are examined in connection to wetland soils and CO_2 fluxes. Wetland soils are typically rich in organic matter due to the slow decomposition rates under anaerobic conditions. These soils frequently contain a high proportion of organic carbon due to the partially degraded plant matter [1]. Wetlands' particular hydrological conditions provide an environment with limited oxygen, which greatly impacts the decomposition rate [2]. It has been extensively proven that wetlands can store carbon. The ability of wetlands to sequester carbon is well-documented. Wetlands account for approximately 30% of the world's terrestrial carbon storage, despite covering only about 6% of the Earth's land surface [3]. The anaerobic environment in wetland soils reduces microbial activity, slowing down decomposition and allowing organic matter to accumulate [4]. This accumulation over time leads to significant

* Corresponding author: dkrcontrol@yahoo.com

carbon sequestration.

While wetlands are carbon sinks, they can also be sources of CO_2 emissions under certain conditions. The balance between carbon sequestration and CO_2 emissions depends on factors like temperature, water levels and human impact [5]. Elevated temperatures can increase microbial activity, accelerating decomposition and leading to higher CO_2 emissions [6]. Similarly, changes in water levels can affect the aerobic or anaerobic conditions in wetland soils, with implications for CO_2 fluxes [7]. Restoration and conservation efforts are critical in maintaining the carbon sequestration functions of wetlands. Restoring degraded wetlands, through re-flooding and reestablishing native vegetation, can help reestablish anaerobic conditions and reduce CO_2 emissions [8, 9]. Water management practices, such as maintaining appropriate water levels, are crucial in preventing aerobic decomposition [10].

To simulate the complex interactions that occur in wetland ecosystems, the DeNitrification-DeComposition (DNDC) model is an essential tool in the field of biogeochemical modeling [11]. The model's core strength lies in its detailed representation of soil carbon and nitrogen dynamics, which are crucial for understanding greenhouse gas emissions [12]. By integrating advanced soil physics, hydrology and plant growth dynamics, it enables accurate simulations of ecosystem responses to environmental change and management practices [13]. The model's ability to simulate the impacts of land-use changes, climate variability and agricultural practices on greenhouse gas emissions has made it an invaluable tool pentru implementarea celor mai bune masuri [14]. The model has been applied to diverse terrestrial ecosystems, demonstrating its ability to capture the complex feedback mechanisms between soil moisture, nutrient dynamics and plant growth [15]. However, its performance in wetland environments, where soil moisture regimes can be highly variable and influenced by multiple stressors, has not been extensively explored [16].

In this study, we evaluated the performance of the DNDC model with input calibration based on measurements of soil characteristics, vegetation type, SOC content and soil moisture regime. Additionally, emission levels were simulated under the most extreme climate change scenario based on Representative Concentration Pathways (RCP) 8.5, to evaluate the possible impact of long-term CO_2 emission trajectories.

Materials and methods

The two study areas are located within the Dambovita River, in Chiajna, a suburban area of Bucharest. In-situ measurements of CO_2 fluxes from the soil surface were conducted in 2022 and were performed monthly. Figure 1 depicts the research locations chosen based on the vegetation that covered them and the soil moisture regime.

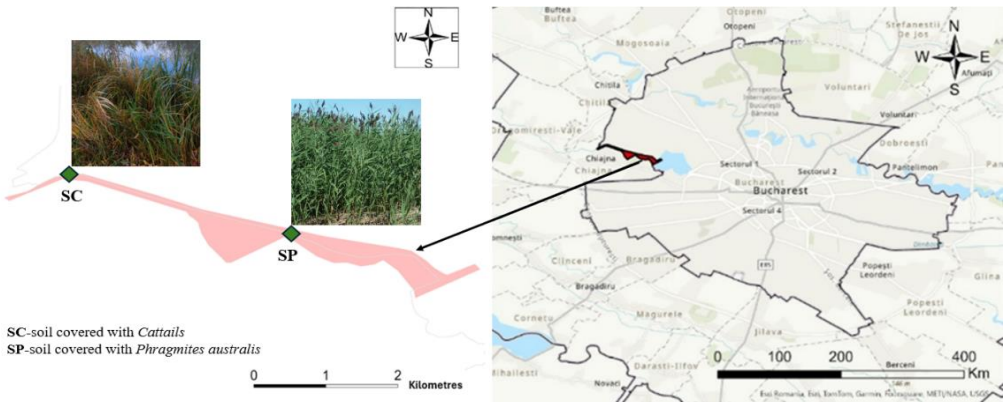

Fig. 1. Spatial representation of the in-situ measurement plots

Thus, in the research area, two types of soil were identified: potentially flooded and flooded soil, as well as two types of wetland vegetation, *Cattails* and *Phragmites australis*. Crop management practices were not applied in the two study areas and there was no known history of manure application before the commencement of the study. The soil in the upstream area (SC) (44°27'53.4"; 25°58'37.7") is characterized by silt loam soil with an average pH of 7.42 and is dominated by *Cattails* vegetation. From the water management perspective, this is flood-prone soil, however, it was not flooded by river waters throughout the measuring period. The second type of soil selected for monitoring is located downstream (44°27'43.5"; 25°59'45.1") and is characterized by *Phragmites australis*-dominated vegetation (SP). The moisture regime varied throughout the year. It was dry from January to July, with humidity values ranging from 11.6% to 45.6% and flooded from August to December.

The climatic context for the current climatology of the study area derives from the observed data and shows a continuous trend of increasing the surface temperature (2m), despite the natural variation. The air temperature and precipitation dynamics used in this study are shown in figure 2.

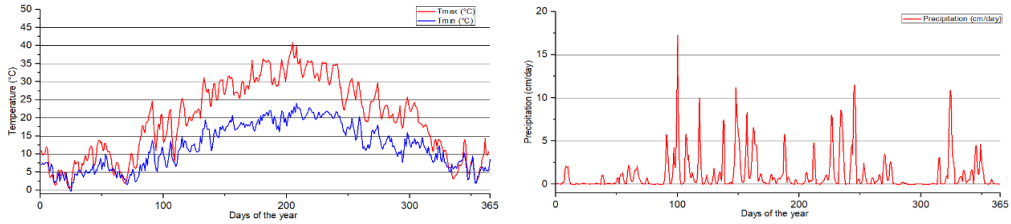

a) b)

Fig. 2. Annual dynamics of daily air temperature at 2m (a) and precipitation (b) in the study area in 2022

The study utilised the process-based biogeochemical model Denitrification-Decomposition (DNDC) (version 9.5) [17] to analyze the dynamics of carbon (C), methane (CH_4) and nitrogen (N) in the wetlands ecosystem in the research location. It integrates daily climate data, soil properties, hydrological features and biogeochemical processes measured and observed in 2022 and accounts for factors such as soil moisture, temperature, organic matter and vegetation to estimate the gas fluxes.

For simulating how changes in GHG emissions might influence various environmental processes within DNDC models, the most common pathways, representing a different level of radiative forcing by the year 2100 can be applied [18]. A low emissions scenario with significant mitigation efforts, aiming to keep global warming below 2°C is RCP 2.6, intermediate stabilization scenarios with moderate levels of emissions reduction are RCP 4.5 and RCP 6.0 and a high emissions scenario with continued increases in greenhouse gas concentrations is RCP 8.5 [19-21].

DNDC simulations using the RCP 8.5 scenarios were conducted to project CO_2 emissions for the years 2050 and 2100, in the context of climate change. RCPs serve as standardized scenarios used to represent different potential futures of greenhouse gas emissions and concentrations, thus providing invaluable insights into the range of possible climate outcomes [22]. These simulations provide insights into potential future emissions under a high greenhouse gas concentration trajectory, helping to understand the long-term impact of climate change on carbon dynamics.

The model input data (climate, soil and management practices) are listed in Table 1. Daily values of atmospheric temperature and precipitation were retrieved from the Baneasa meteorological station. The soil parameters were based on the results of field studies. The cultivation period was designated between March 1st and October 30th for all SC crop practices and between April 15th and September 30th for SP. The fraction of leaves and stems left in the

field after harvest was considered to be 100%.

Table 1. Details of the input data for the model predictions

Data Type	Sub-Type	Unit	Model Prediction	
			SC soil	SP soil
Climate	Temperature	°C	Daily values for 2022 RCP 8.5 for 2050, 2100	
	Precipitation	Cm		
Management practices	Fertilization	kg N ha^{-1}	Auto-fertilization	
	Tillage	Cm	N/A	
Soil	Bulk density	g cm^{-3}	1.07191	1.5078
	Clay	%	14	63
	Initial SOC	kg C/kg soil	0.00274	0.00638
	pH		7.42	6.21

The method applied to assess emissions at the soil-atmosphere interface is based on directly measuring CO_2 fluxes inside a chamber with a known surface area [23], which was conducted using a portable infrared CO_2 gas analyzer (EGM-5) presented in figure 3. The method used is dynamic, relying on monitoring the variations in concentration of carbon dioxide (ppm) between air entering and leaving the chamber [24]. Soil respiration (kg C/ha/day) was calculated by tracking the rate of change in the concentration of CO_2 inside the chamber over a 60-second period.

Fig. 3. CO_2 flux analyzer with a closed dynamic chamber

The DNDC model's performance was evaluated based on in-situ CO_2 emission measurements and goodness of fit indicators: relative bias in percent (RBP), the Nash-Sutcliffe efficiency coefficient (NSE) and mean absolute error (MAE). PBIAS measures the overall bias of the model by indicating whether the simulated values tend to be higher or lower than the observed data [25]. The NSE evaluates the model's predictive accuracy [26], while MAE, on the other hand, represents the average magnitude of errors between the simulated and observed values, calculated as the mean of the absolute differences between them [27].

$$RBP = \frac{\Sigma_{i=1}^{n}(sim_i - obs_i)}{\Sigma_{i=1}^{n} obs_i}; NSE = 1 - \frac{\sum_{i=1}^{n}(obs_i - sim_i)^2}{\sum_{i=1}^{n}(obs_i - \overline{obs})^2}; MAE = \frac{\Sigma_{i=1}^{n}|sim_i - obs_i|}{n} \quad (1)$$

where: sim_i represents the forecast value and obs_i represents the observation value.

The combined use of these metrics provides a comprehensive assessment, confirming that the model accurately captures the dynamics of carbon emissions with minimal bias and acceptable error margins, ensuring the reliability of the simulation results.

Results and discussion

The graphs in Figure 4 provide a comprehensive daily breakdown of the CO_2 fluxes from the soil-atmosphere interface, observed and measured during the year 2022 in the locations SC (Fig. 4a)) and SP (Fig. 4b)).

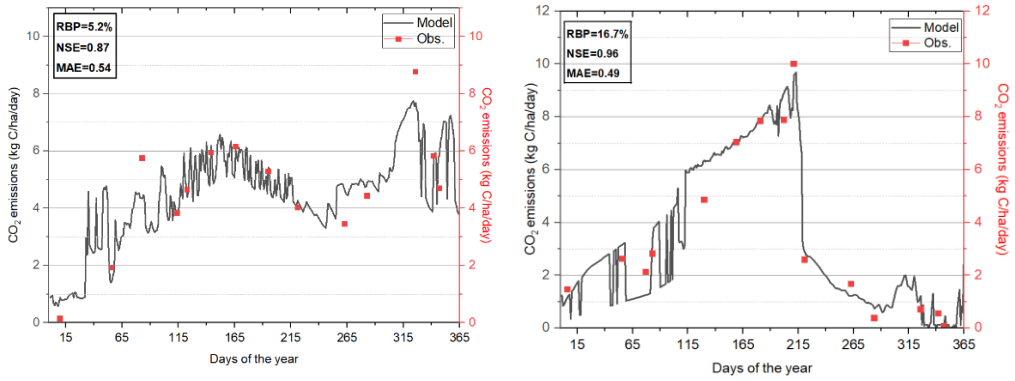

Fig. 4. Interannual variations of soil CO_2 emission fluxes observed and modelled for SC (a) and SP (b)

Fluxes are minimal in the winter, when biological activity naturally reduces, which reflects the slower rate of these processes. Consequently, during the winter season, the daily simulated CO_2 emissions for the SC location ranged from 0.88 to 5.83kg CO_2-C ha^{-1} d^{-1}, whereas the observed values ranged from 0.14 to 5.81kg CO_2-C ha^{-1} d^{-1}. In the SP location, the simulated values for the winter season ranged from 0.12 to 3.17kg CO_2-C ha^{-1} d^{-1}, while the values measured in-situ were between 0.07 and 2.61kg CO_2-C ha^{-1} d^{-1}. In contrast, the growing season is characterized by significant fluctuations in greenhouse gas emissions as biological activity intensifies. The simulated values of the model for the SC location, between 3.77 and 6.19kg CO_2-C ha^{-1} d^{-1} are closely correlated with the measured values between 3.82 and 6.15kg CO_2-C ha^{-1} d^{-1} and highlight this seasonal dynamic, providing an insight into how CO_2 emissions vary throughout the year. The model tends to overestimate CO_2 emissions compared to the measured values in the SP location throughout the growing season and peak emission period; nonetheless, the model corresponds to the observed data.

The key performance metrics for SC and SP show distinct differences in their predictive accuracy and performance. SC has a relatively lower RBP (5.2%) compared to SP (16.7%), indicating SC's predictions are closer to the observed values. However, SP's higher NSE (0.96) compared to SC's (0.87) suggests that SP's model explains more of the variability in the data, reflecting a better fit overall. Both models have similar MAE values, with SC at 0.54 and SP at 0.49, indicating that the average magnitude of prediction errors is quite close. While SP demonstrates a better fit and slightly lower error, SC's lower RBP suggests it may have more accurate predictions relative to its observed values.

The comparison of the measured fluxes with field measurement data through these performance metrics shows that, while the model slightly overestimates the emissions in the two locations, it fits well in simulating the observed data.

The seasonal variation in CO_2 emissions among different ecosystem components for locations SC and SP are presented in figure 5 and reveal distinct patterns.

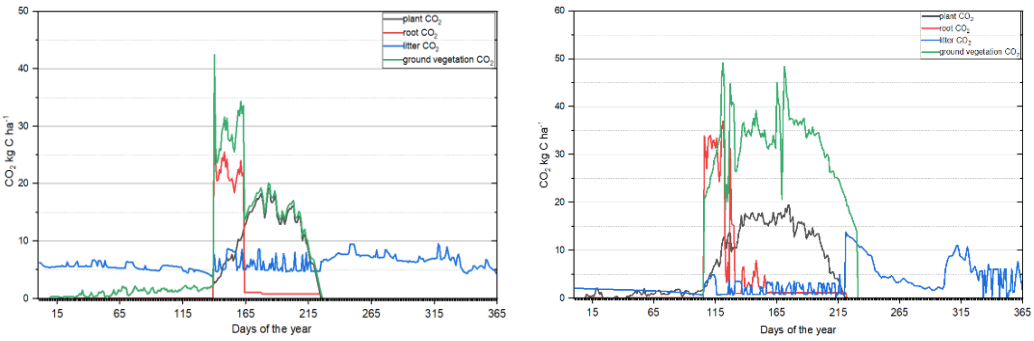

Fig. 5. Composite modelled CO_2 fluxes of the SC (a) and SP (b) over 2022

The plant CO_2 emissions shows significant fluctuations, with notable peaks around the vegetation season for both locations, indicating periods of high photosynthetic activity or plant respiration. Root CO_2 shows a sharp peak for the SC location between days 130-165, suggesting intense root respiration during the growing season, while for the SP location it shows a similar period of increased emissions followed by a decrease, reflecting short root activity. In the SP location, emissions from this ecosystem component indicate a stable trajectory until the period of soil flooding, when a steep increase was observed, followed by notable variations, reflecting the decomposition of organic matter under flooding conditions. In contrast, emissions from litter CO_2 in the SC location remain relatively stable with slight increases. The emissions from ground vegetation show a seasonal pattern for both locations, with higher emissions during the warmer months. In location SC, the peak correspond to the early summer period when vegetation activity is typically higher due to favorable weather conditions. CO_2 emissions from ground vegetation at the SP site also peak early but decline more steadily, indicating a later end to active growth.

Impacts of climate change on GHGs emissions

Under RCP 8.5 climate change scenario, CO_2 emissions from both locations are significantly higher in 2050 and 2100 compared to the baseline which represents the reference level of CO_2 emissions from 2019-2023. According to figure 6a, the model for top-soil emissions from the SC location predicts an increase of 16.79 % until 2100. Emissions for 2050 and 2100 generally follow the baseline model, but with some notable differences, where the peaks in 2100 are generally higher than those in the baseline and 2050, which might suggest changes in soil composition, microbial activity, or environmental conditions affecting CO_2 emissions.

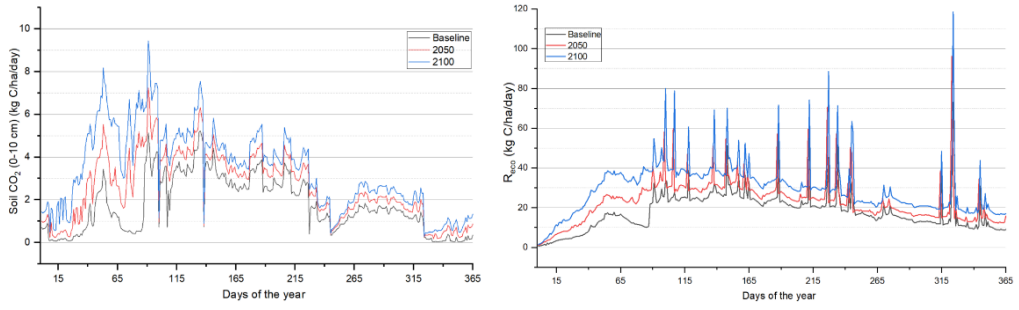

Fig. 6. Topsoil emissions (a) and ecosystem respiration (b) simulated according to RCP 8.5 scenarios for the SC location

The graph in figure 6b shows the ecosystem's respiration rate variability model (R_{eco}) for the SC location according to scenarios for 2050 and 2100. R_{eco} simulated for 2050 and 2100 follow a similar pattern, with particularly pronounced peaks that appear to be seasonal and

troughs occurring around the same days throughout the year. The 2100 scenario exhibits higher peaks than Baseline and 2050, indicating an increase in rate over time, with occasional spikes significantly higher than the general trend.

According to the same RCP 8.5 scenario, the model predicted the CO_2 emissions from top-soil atmosphere interface and R_{eco} for SP location, as shown in figure 7. The scenarios have been conducted here without considering periodic or permanent soil flooding events. The model for CO_2 emissions predicts an increase of 14.02 % until 2100. The more pronounced difference between the simulations for 2100 compared to the baseline and 2050 is observed before the vegetation period, between days 50 and 110, when higher peaks are simulated. The model for the variability of R_{eco} follows a similar pattern for the analyzed scenarios. In comparison to Baseline and 2050, the 2100 scenario shows higher peaks, suggesting a gradual increase in rate with intermittent increases that are noticeably higher than the overall trend.

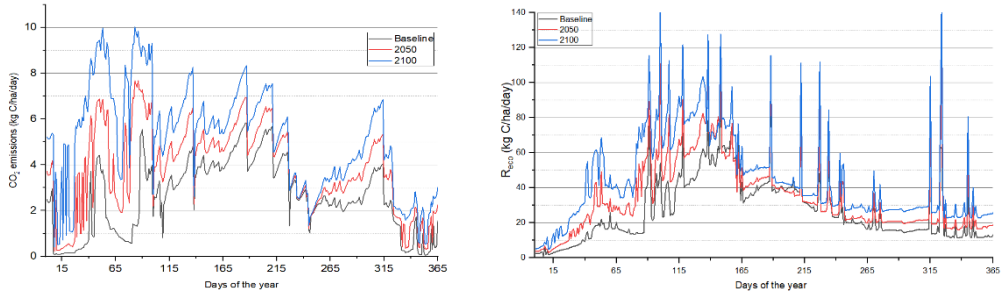

Fig. 7. Topsoil emissions (a) and ecosystem respiration (b) simulated according to RCP 8.5 scenarios for the SP location

The Table 2 presents greenhouse gas emissions under two different scenarios (SC and SP) for baseline conditions, as well as projections for 2050 and 2100. CO_2 emissions are projected to increase across both scenarios, with SC showing a rise from 5960.01kgC/ha/yr at baseline to 7215.35kgC/ha/yr by 2100, while SP shows a higher increase from 7405 kgC/ha/yr at baseline to 8443.45kgC/ha/yr by 2100.

Table 2. Model outputs for SC and SP areas and greenhouse gas (GHG) emissions for each of the two scenarios (2050,2100 under the RCP 8.5 projection)

Model Outcome		**GHGs Emissions**					
	Unit	**SC**			**SP**		
Scenario		Baseline	2050	2100	Baseline	2050	2100
CO_2 emissions	kgC/ha/yr	5960.01	6960.91	7.215.35	7405	8091	8443.45
CH_4 emissions	kgC/ha/yr	-1.67	-1.86	-2.09	18.24	-0.42	-0.49
N_2O	kgN/ha/y	12.92	15.78	17.6	0.63	29.48	36.59
NO	kgN/ha/y	0.13	0.39	0.42	0.05	0.46	0.52
N_2	kgN/ha/y	0.41	0.9	0.99	0.12	2.68	3.2
NH_3	kgN/ha/y	22.1	36.54	38.33	53.15	59.92	66.12
*Baseline							

Interestingly, CH_4 emissions under SC decrease slightly over time, shifting from -1.67kgC/ha/yr at baseline to -2.09kgC/ha/yr by 2100, while SP sees a significant reduction from 18.24kgC/ha/yr at baseline to -0.49kgC/ha/yr by 2100. N_2O and other nitrogen-related emissions, such as NO, N_2 and NH_3, generally show an increasing trend across both scenarios, with SP indicating a more pronounced rise, especially in N_2O emissions, which jump from 0.63kgN/ha/yr

at baseline to 36.59kgN/ha/yr by 2100. These results highlight the potential for significant changes in greenhouse gas emissions over the century, varying notably between scenarios.

Conclusions

The results present significant findings regarding the dynamics of carbon emissions in wetland ecosystems, particularly using the DeNitrification-DeComposition (DNDC) model. In-situ measurements of CO_2 fluxes were conducted monthly in 2022, validating the model simulations through statistical analysis of uncertainties. The comparative analysis between the SC and SP locations reveals differences in model performance. While the SC location shows a lower relative bias percentage (RBP) of 5.2%, indicating closer alignment with observed values, the SP location demonstrates a higher Nash-Sutcliffe efficiency (NSE) of 0.96, reflecting a better overall fit to the data. Despite these differences, both models exhibit similar mean absolute errors (MAE) for SC and SP of 0.54 and respectively 0.49, indicating that prediction errors are consistent across locations. This balance between accuracy and fit underscores the utility of the DNDC model in capturing the complexities of CO_2 emissions in different wetland environments. Thus, the results showed consistency between DNDC outputs and field measurements, improving the confidence in the model's application for assessing wetland ecosystems.

The analysis revealed that CO_2 fluxes are highly sensitive to temperature and soil moisture/flooding conditions. The SP location provides support for the correlation between soil flooding and CO_2 emissions, since the monitoring year's CO_2 emissions were significantly decreased due to flooding that occurred in August.

The model's forecast under RCP 8.5 scenario for both the SC and SP locations indicates substantial increases in CO_2 emissions by 2100 compared to baseline levels (2019-2023). The SC location shows a predicted increase of 16.79% in top-soil emissions by 2100 and for SP location was predicted an increase of 14.02%. This pattern indicates that changes in seasonal dynamics, such as shifts in the timing and intensity of biological processes, could significantly influence carbon emissions. The absence of flooding events in the model simulations further emphasizes the sensitivity of these ecosystems to climatic variables.

As these models indicate significant rises in emissions by 2100, future perspectives will focus on improving the accuracy of simulations and integrating more detailed data on local climate variations and biogeochemical processes to enhance predictive capabilities.

Acknowledgments

This work was carried out through the Nucleu Program (44N/2023) within the National Plan for Research, Development and Innovation 2022-2027, supported by the Romanian Ministry of Research, Innovation and Digitization, project PN 23 31 04 01/2023.

References

[1] S.D. Bridgham, J.P. Megonigal, J.K. Keller, N.B. Bliss, C. Trettin, *The carbon balance of North American wetlands*, **Wetlands**, **26**(4), 2006, pp. 889–916. DOI: 10.1672/0277-5212(2006)26[889:TCBONA]2.0.CO;2.

[2] R.A. Chimner, B.D. Murdock, S.M.H. Shafer, J.M. Crozier, L.I. Juri, D.A. Cooper, K.R. Wright, W.A. Reiners, *Carbon stock estimations for various wetlands across the United States,* **Wetlands**, **37**(2), 2017, pp. 487–496.

[3] W.J. Mitsch, J.G. Gosselink, **Wetlands**, 5th Edition, John Wiley & Sons, Inc., Hoboken, 2015.

[4] B. Kayranli, M. Scholz, A. Mustafa, Å. Hedmark, *Carbon storage and fluxes within freshwater wetlands: a critical review,* **Wetlands**, **30**(1), 2010, pp. 111–124. DOI: 10.1007/s13157-009-0003-4.

[5] T. Ise, A.L. Dunn, S.C. Wofsy, P.R. Moorcroft, *High sensitivity of peat decomposition to climate change through water-table feedback,* **Nature Geoscience**, 1(11), 2008, pp. 763–766. DOI: 10.1038/ngeo331.

[6] T.R. Moore, R. Knowles, *Methane Emissions from Fen, Bog and Swamp Peatlands in Quebec*, **Biogeochemistry, 11**(1), 1990, pp. 45-61.

[7] J.T. Verhoeven, T.L. Setter, *Agricultural use of wetlands: opportunities and limitations,* **Annals of Botany, 105**(1), 2010, pp. 155-163. DOI: 10.1093/aob/mcp172.

[8] N. Enache, L. Laslo, G. Deák, M. Matei, M. Boboc, S.Y. Yusuf, *Seasonal Sensitivity of Reco from Aquatic Ecosystem to Meteorological and Physicochemical Water Parameters*, **E3S Web of Conferences**, **437**, 2023, Article Number: 02012. DOI: 10.1051/e3sconf/202343702012.

[9] S.E. Page, R.A.J. Wüst, D. Weiss, J.O. Rieley, W. Shotyk, S.H. Limin, *Global and regional importance of the tropical peatland carbon pool*, **Global Change Biology**, **17**(3), 2011, pp. 798–818. DOI: 10.1111/j.1365-2486.2010.02279.x.

[10] Y. Zhang, C. Li, C. Trettin, H. Li, G. Sun, *An integrated model of soil, hydrology, and vegetation for carbon dynamics in wetland ecosystems*, **Global Biogeochemical Cycles**, **16**(4), 2002, Article Number: 1061. DOI: 10.1029/2001GB001838.

[11] C. Li, S. Frolking, T.A. Frolking, *A model of nitrous oxide evolution from soil driven by rainfall events: 1. Model structure and sensitivity*, **Journal of Geophysical Research - Atmospheres**, **97**(D9), 1992, pp. 9759–9776. DOI10.1029/92JD00509.

[12] J. Deng, C. Li, S. Frolking, *Modeling impacts of changes in temperature and water table on C gas fluxes in an Alaskan peatland*, **Journal of Geophysical Research - Biogeosciences**, **120**(7), 2015, pp. 1279–1295. DOI: 10.1002/2014JG002880.

[13] J. Perlman, R.J. Hijmans, W.R. Horwath, *Modelling agricultural nitrous oxide emissions for large regions*, **Environmental Modelling & Software**, **48**, 2013, pp. 183–192. DOI: 10.1016/j.envsoft.2013.07.002.

[14] M. Abdalla, A. Hastings, M. Helmy, A. Prescher, B. Osborne, G. Lanigan, D. Forristal, D. Killi, P. Maratha, M. Williams, K. Rueangritsarakul, P. Smith, P. Nolan, M.B. Jones, *Assessing the combined use of reduced tillage and cover crops for mitigating greenhouse gas emissions from arable ecosystem*, **Geoderma**, **223**, 2014, pp. 9–20. DOI: 10.1016/j.geoderma.2014.01.030.

[15] H. Vereecken, A. Schnepf, J.W. Hopmans, M. Javaux, D. Or, D.O.T. Roose, J. Vanderborght, M.H. Young, W. Amelung, M. Aitkenhead, S.D. Allison, S. Assouline, P. Baveye, M. Berli, N. Bruggemann, P. Finke, M. Flury, T. Gaiser, G. Govers, T. Ghezzehei, P. Hallett, H.J. Hendricks Franssen, J. Heppell, R. Horn, J.A. Huisman, D. Jacques, F. Jonard, S. Kollet, F. Lafolie, K. Lamorski, D. Leitner, A. McBratney, B. Minasny, C. Montzka, W. Nowak, Y. Pachepsky, J. Padarian, N. Romano, K. Roth, Y. Rothfuss, E.C. Rowe, A. Schwen, J. Šimůnek, A. Tiktak, J. Van Dam, S.E.A.T.M. van der Zee, H.J. Vogel, J.A. Vrugt, T. Wöhling, I.M. Young, *Modeling soil processes: review, key challenges, and new perspectives*, **Vadose Zone Journal, 15**, 2016, pp. 1–57. DOI: 10.2136/vzj2015.09.0131.

[16] M.R. Turetsky, B.W. Benscoter, S. Page, G.R. Rein, G.J. van der Werf, A. Watts, *Global vulnerability of peatlands to fire and carbon loss,* **Nature Geoscience**, **8**(1), 2015, pp. 11–14. DOI: 10.1038/NGEO2325.

[17] *** * ***, http://www.dndc.sr.unh.edu/ [accessed on: 30.02.2024]

[18] D.P. van Vuuren, J. Edmonds, M. Kainuma, K. Riahi, A. Thomson, K. Hibbard, S.K. Rose, *The representative concentration pathways: An overview*, **Climatic Change**, **109**(1), 2011, pp. 5–31. DOI:10.1007/s10584-011-0148-z.

[19] T.F. Stocker, D. Qin, G.K. Plattner, M. Tignor, S.K. Allen, J. Boschung, P.M. Midgley, **Climate Change 2013: The Physical Science Basis**, Cambridge University Press, 2013.
[20] * * *, **Climate Change 2014: Synthesis Report. Contribution of Working Groups I, II and III to the Fifth Assessment Report of the Intergovernmental Panel on Climate Change** [Core Writing Team, R.K. Pachauri and L.A. Meyer (eds.)], IPCC, Geneva, Switzerland, 2014, 151p.
[21] R.H. Moss, J.A. Edmonds, K.A. Hibbard, M.R. Manning, S.K. Rose, D.P. van Vuuren, T.J. Wilbanks, *The next generation of scenarios for climate change research and assessment*, **Nature**, **463**(7282), 2010, pp. 747–756. DOI:10.1038/nature08823.
[22] M. Meinshausen, S.J. Smith, K. Calvin, J.S. Daniel, M.L. Kainuma, J.F. Lamarque, D.P. van Vuuren, *The RCP greenhouse gas concentrations and their extensions from 1765 to 2300*, **Climatic Change**, **109**(1-2), 2011, pp. 213–241. Special Issue: SI. DOI: 10.1007/s10584-011-0156-z.
[23] * * *, www.ppsystems.com [accessed on: 07.04.2024]
[24] L. Laslo, M. Matei, M. Boboc, Gy. Deák, I. Cătuneanu, N. Enache, and N. Rahim, Measurements and Statistical Analysis of CO_2 Efflux and Related Parameters from Crop and Forested Lands, **E3S Web Conf.**, vol. 1216, 2023. DOI: https://doi.org/10.1051/e3sconf/202343702012.
[25] D. N. Moriasi, M. W. Gitau, N. Pai, P. Daggupati, *Hydrologic and water quality models: Performance measures and evaluation criteria*, **Transactions of the ASABE**, **58**(6), 2015, pp. 1763–1785. DOI:10.13031/trans.58.10715.
[26] J.E. Nash, J.V. Sutcliffe, *River flow forecasting through conceptual models part I—A discussion of principles,* **Journal of Hydrology**, **10**(3), 1970, pp. 282–290. doi:10.1016/0022-1694(70)90255-6.
[27] C.J. Willmott, K. Matsuura, Advantages of the mean absolute error (MAE) over the root mean square error (RMSE) in assessing average model performance, **Climate Research**, **30**(1), 2005, pp. 79–82. DOI: 10.3354/cr030079.

Received: May 12, 2024
Accepted: September 10, 2024